# Thermal Properties Relevant to the Processing of PET Fibers

**K. De Clerck,[1] H. Rahier,[2] B. Van Mele,[2] P. Kiekens[1]**

[1]*Department of Textiles, Ghent University (UGent), Technologiepark 907, 9052 Ghent, Belgium*
[2]*Department of Physical Chemistry and Polymer Science, Free University of Brussels (VUB), Pleinlaan 2, 1050 Brussels, Belgium*

Received 24 July 2002; accepted 2 January 2003

**ABSTRACT:** The thermal properties of poly(ethylene terephthalate) (PET) conventional fibers and microfibers are measured and compared to bulk samples. It is shown that the glass transition temperature ($T_g$) of the fibers can be monitored with modulated differential scanning calorimetry (MDSC). The $T_g$ region is about 30°C wide and shifted to approximately 110°C for conventional as well as for micro-PET fibers. The $T_g$ of these fibers is compared to the $T_g$ of cold-crystallized bulk samples. Upon crystallization, a shift and even a split up of $T_g$ is observed. The second $T_g$ is much broader and is situated around 90°C. This $T_g$ is related to the appearance of a rigid amorphous phase. In comparison, the mobility of the amorphous phase in fibers is even more restricted. The whole multiple melting profile observed on the fibers is the result of a continuous melting and recrystallization process, in contrast to bulk PET. The heat-set temperature is shown to trigger the start of melting and recrystallization. It is seen in the MDSC as an exotherm in the nonreversing signal and an excess contribution in the heat-capacity signal. © 2003 Wiley Periodicals, Inc. J Appl Polym Sci 89: 3840–3849, 2003

**Key words:** glass transition; fibers; polyesters; differential scanning calorimetry (DSC); thermal properties

## INTRODUCTION

Poly(ethylene terephthalate) (PET) fibers are a worldwide-favored material for the production of textiles. The ongoing tendency to move to increasingly finer fibers led to the introduction of microfibers in the beginning of the 1990s (for PET fibers, this implies a fiber diameter smaller than or equal to 10 $\mu$m, compared to, for example, 25 $\mu$m for a typical conventional PET textile fiber). The use of microfibers results in superior properties of the fabrics, such as an improved drape and silky feeling and an improved water repellence while retaining breathability. However, the increased fineness also results in a more critical processing, with the major drawback of PET microfibers being their bad dyeing performance.[1–7]

Dye application in PET dyeing is well-established industrially as a result of the many years of practical experience in dyeing. Both conventional and microfiber PET fabrics are commonly dyed with disperse dyes in pressurized vessels at 130°C. In contrast, a fundamental understanding of the mechanisms by which dyes are absorbed by fibers is still not completely achieved. With the introduction of ever-finer PET fibers for the production of textile fabrics, the general need for a basic understanding of the relation between fiber and dyeing properties has become vital. Indeed, for the fine fibers and the newer microfibers, in particular, problems in achieving a uniform color buildup are more evident and require, thus, fundamental scientific knowledge of dyeing kinetics and equilibria to achieve commercial acceptability and to allow further process and product development. The fiber thermal properties of importance in the understanding of the dyeing mechanisms are the glass transition region and the start of the melting and recrystallization process.

The glass transition of fibers is a vital parameter for optimizing the dyeing process, as it is generally accepted that the dyeing temperature needs to be above the glass transition temperature ($T_g$) for the amorphous phase to become mobile and to enable an efficient diffusion of the dye into the fiber with subsequent good color buildup. Although this has long been recognized in textiles,[8–11] little is known about a direct method for determining the fiber $T_g$.

The melting of bulk PET is widely discussed in the literature using both conventional and modulated differential scanning calorimetry (DSC),[12–20] but, again, little is known specifically on the melting of PET fibers. The start of the melting and recrystallization process demands further research as the dyeing or any

*Correspondence to:* K. De Clerck (karen.declerck@ugent.be).
Contract grant sponsor: European Commission; contract grant number: BRPR-CT98-0793.
Contract grant sponsor: Ghent University; contract grant sponsor: 011D5495.

further textile process temperature (such as the application of a coating onto the fabric) needs to stay well below this start temperature to ensure the dimensional stability of the fabric. For this purpose, a heat-set process is introduced prior to dyeing, as it improves the dimensional stability during the dyeing process. This is usually performed by exposing the fabrics in a stenter to a temperature in between the dyeing temperature and the melting temperature ($T_m$), typically 180–190°C, as to allow the fabrics a predefined and controlled shrinkage. The heat-set process is an annealing treatment that may affect the original morphology of the fibers and, as such, also their thermal properties as well as their dyeing properties.

It is clear that the study of the thermal properties of fibers is important for the understanding of the dyeing process. Further, the thermal transitions may very well be altered by the specific conditions of the heat-set process. However, until now, in textiles, dyeing temperatures and other process parameters are usually determined empirically without trying to understand the relationship with the thermal properties of the fibers.

In this article, modulated differential scanning calorimetry (MDSC) was used for the determination of the fiber $T_g$ and for investigating the interrelation between the fiber $T_g$ and the dyeing process. The fiber $T_g$ was also rationalized by comparing it to the $T_g$ of a series of bulk (nonfibrous) PET samples. The melting of PET fibers was looked at by both conventional DSC and MDSC and compared with the literature on bulk PET. Further a series of PET fabrics heat-set at different temperatures was investigated to determine the influence of the heat-set temperature on the glass and melting transition regions of the fibers. Finally, this knowledge will be used in a following article[21] to investigate the interrelation between the dyeing with disperse dyes varying in chemical structure and the thermal properties of PET fibers.

## EXPERIMENTAL

### Materials

Sofinal (Waregem, Belgium) supplied all the fabrics, consisting of PET fibers only. The supplied fabrics were all thoroughly washed and dried, to remove all sizing agents and other auxiliaries. In addition, they were subjected to a heat-set treatment to impart dimensional stability during the dyeing process. Heat-setting was performed on a stenter. Drying was also performed on a stenter, but in contrast to the heat-setting, the fabrics were introduced wet and the processing time and temperature were not as well controlled.

The two standard fabrics used were fabric qualities 6460 and 6145. Quality 6460 is a conventional fiber fabric in which warp and weft consist of the same 167/30 yarn (the yarn count is 167 dtex and the yarn consists of 30 filaments). A single fiber or filament thus has a linear density of 5.6 dtex, an approximate diameter of 23–24 $\mu$m, and a circular cross section. The fabric was heat-set at 190°C for 30 s. This fabric will be referred to as the conventional fiber fabric.

Quality 6145 is a microfiber fabric in which the weft is a 100/176 yarn, and the warp, a 76/136 yarn. Single weft and warp fibers thus have a linear density of 0.57 and 0.56 dtex, respectively, and an approximate diameter of 7–7.5 $\mu$m. The warp fibers have a circular cross section, and the weft fibers, a hexagonal cross section. The fabric was heat-set at 180°C for 30 s. This fabric will be referred to as the microfiber fabric.

To study the effect of the heat-set treatment in more detail, a further three fabric qualities (6645, 6447, and 5065) were supplied by Sofinal. Of each fabric quality, four different samples were supplied: a sample that was not heat-set and three samples heat-set at temperatures of 180, 200, and 220°C, respectively. All samples were dried at a temperature to 140°C prior to the possible subsequent heat-setting.

Quality 6645 consists of a 110/192 weft yarn (fiber linear density of 0.57 dtex) and an 83/72 warp yarn (fiber linear density of 1.15 dtex). Quality 6447 consists of a 330/96 weft yarn (fiber linear density of 3.44 dtex) and a 167/48 warp yarn (fiber linear density of 3.48 dtex). Quality 5065 consists of a 167/48 weft yarn (fiber linear density of 3.48 dtex) and a 55/24 warp yarn (fiber linear density of 2.29 dtex). These fabrics will be referred to by their quality number.

As warp and weft did not consist of the same yarn for most of the fabrics investigated, and even if they would, they may have a slightly different morphology, due to the high periodic tensions applied on the warp yarns during the weaving process, warp and weft were separated before analyses with MDSC. This also eliminated the possible introduction of local stresses in the sample during the DSC run due to fiber entanglement in the fabric. Unless otherwise stated, the reported figures relate to the weft fibers of the fabrics. The warp fibers, however, gave similar results and led to the same conclusions.

To obtain fully amorphous bulk PET samples, the weft fibers of the conventional fabric were heated at 280°C for 5 min and quenched in liquid nitrogen. The results reported on these samples were the same as on a fully amorphous PET sample, prepared in a similar manner but starting from PET pellets purchased from Aldrich (Ontario, Canada). The series of semicrystalline bulk PET samples studied in Figure 4 were obtained by annealing the amorphous bulk PET samples at 100°C for various times. The semicrystalline bulk PET samples described in the other figures are the conventional PET fiber after cooling from the melt at 20°C/min.

### DSC and MDSC

DSC and MDSC measurements were performed in nonhermetic aluminum pans on a TA Instruments DSC 2920 with an MDSC® option, using an underlying heating rate of 2°C/min unless otherwise stated. The purge gas was nitrogen (25 mL/min). The temperature was calibrated with gallium, indium, and tin. Indium was used for enthalpy calibration. For the modulated experiments, a 2°C modulation amplitude for the fibers, a 1°C modulation amplitude for the bulk samples, and a 60-s modulation period was used. The heat capacity (*Cp*) was calibrated with poly(methyl methacrylate), using the same modulation conditions as in the experiments.

The high modulation amplitudes used were necessary to obtain an acceptable signal-to-noise ratio for the very weak and broad glass transitions studied. The derivative of the heat capacity (*dCp/dT*) signal was used to optimize the modulation amplitude. Modulation amplitudes of 0.3–2°C were considered with a 60-s modulation period and a 2°C/min underlying heating rate. Using still larger modulation amplitudes or shorter modulation periods may cause distortion of the sine wave and is therefore not recommended. For the fibers, a modulation amplitude of 2°C shows the lowest noise and was chosen for further study, while for the bulk samples (optimization was performed on the samples with the longest annealing time), a modulation amplitude of 1°C was chosen as no significant difference in noise was observed between the 1 and the 2°C modulation amplitudes and the latter was relatively large compared to the width of the narrower transitions of the samples annealed for shorter times.

Sample masses of 6 ± 0.5 mg were used for the MDSC experiments (mainly to study the glass transition but also the start of melting) and 2.7 ± 0.3 mg for the conventional DSC experiments (to study the melting transition). A sample mass of 2.7 mg fills the bottom of the pan and showed the best reproducible results in the melting transition. Higher masses did not give such a clear separation of the melting peaks. On the other hand, the higher masses of 6 mg (which is about the maximum amount of bulky fibrous sample that could be put into the sample pan) were beneficial to account for the very weak signals in the glass transition region as well as in the start of melting.

The specifications of the glass transition region were calculated using the half-extrapolated tangents option in the TA Instruments software. The glass transition specifications were measured on at least five different experiments for the weft of both the standard conventional fiber and the microfiber fabrics. This resulted in standard deviations of 1.5°C for the $T_g$ and 0.015 J/g/°C for the $\Delta Cp$. The measurements of $T_g$ for the other fibers (warp of the standard fabric qualities and both warp and weft of fabric qualities 6645, 6447, and 5065) were performed at least twice, showing that the trends were reproducible. The determination of the onset of melting and recrystallization was performed at least twice on all samples. Again, the trends were reproducible.

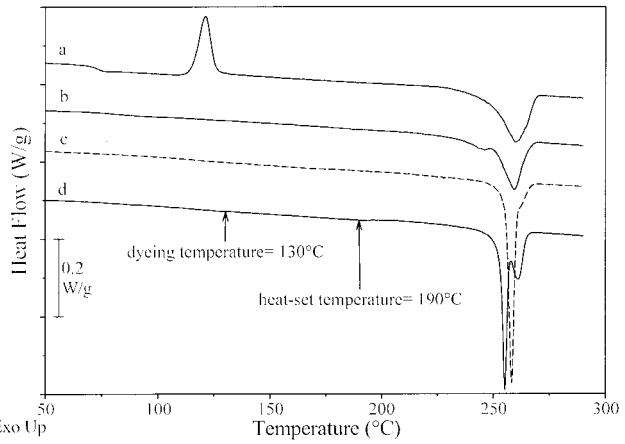


**Figure 1** Conventional DSC on bulk and fibrous PET: (a) amorphous bulk sample; (b) semi-crystalline bulk sample; (c) microfiber; (d) conventional fiber.

In the experimental MDSC conditions of this work, for both the $T_g$ region and the start of the melting region, the variation in the corrected heat-flow phase angle was always limited to a few degrees. The modulus of the complex heat capacity and the in-phase heat-capacity component thus nearly coincide.[22] The term (specific) heat capacity (*Cp*), without further specification, will therefore be used throughout this work.

In the *dCp/dT* signal, a small peak could be observed around 160°C, which was showed to be the result of the Curie transition of the Alumel thermocouple in the DSC cell. Since the transitions looked at in this work are of the same order of magnitude as this interfering signal, the latter was corrected for clarity. The correction was performed by subtracting the signal of a quenched PET sample in this temperature region.

## RESULTS AND DISCUSSION

### Characterization of the glass transition

Figure 1 shows the heat-flow signal obtained by conventional DSC of the weft fibers of the conventional fiber PET fabric and microfiber PET fabric, a semicrystalline bulk PET sample, and a fully amorphous bulk PET sample. The heat-set temperature as well as the dyeing temperature are also shown in Figure 1. Figure 2 zooms in on the glass transition region. Both figures show that conventional DSC can observe no $T_g$ on the fiber samples and that the $T_g$ of the amorphous and semicrystalline bulk PET samples is situated around 70 and 80°C, respectively.

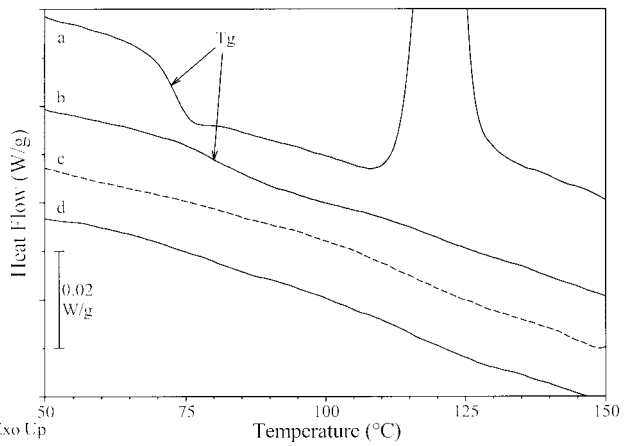


**Figure 2** Glass transition region of bulk and fibrous PET. Conventional DSC. (a) Amorphous bulk sample; (b) semicrystalline bulk sample; (c) microfiber; (d) conventional fiber.

In most of the literature related to the dyeing of PET fibers, the importance of the glass transition is widely accepted,[8–11] but the temperature range of the $T_g$ of PET fibers is often not stated, and if it is, temperatures around 80–90°C are given.[9,11,23] However, no references were found of a direct measurement of the $T_g$ of PET fibers. If the fiber $T_g$ would indeed be situated around 80°C, the dyeing process could be performed at 90–100°C and there would be no need for the generally accepted dyebath temperature of 130°C, which demands costly high-pressure dyeing vessels.

The morphology and thus also the thermal properties of a fiber are different from those of the same polymer material in bulk. Fibers are drawn, texturized, and heat-set, resulting in high percentages of crystallinity as well as high degrees of orientation and mobility restriction in the amorphous phase. In general, a mobility restriction or delayed mobility of the amorphous phase, referred to as rigid amorphous phase, leads to an increase of the average value of the glass transition temperature and a spreading out of the glass transition over a wider temperature range.[24–28]

MDSC is reported to be a sensitive technique to study broad and weak transitions[28–30] and was therefore used in this work to investigate the glass transition region of the PET fibers. Figure 3 shows the heat-capacity (*Cp*) signal of the basic conventional fiber, the microfiber, and the bulk PET samples, obtained by MDSC.

A very broad, weak glass transition can now be observed for the fibers, as well as a shift of the $T_g$ to higher temperatures ($T_g \cong 110$°C) when compared to the bulk PET samples. Table I shows the characteristics of the $T_g$ region for both fibers, measured on the *Cp* signal. The *Cp* signal is most suited for obtaining quantitative information, as the noise level on the *dCp/dT* signal is still considerable in spite of the high amplitudes used. The *dCp/dT* signal, on the other hand, is a useful indicator of the start and end of the very weak glass transitions (Fig. 4).

Song and Hourston already used MDSC to show that bulk semicrystalline PET samples, obtained by cooling from the melt at different cooling rates, result in a broadening of the glass transition and a shift in $T_g$ toward higher temperatures with a slower cooling rate.[28] To rationalize the very broad and weak glass transition at relatively high temperatures for the PET fibers observed in this work, it was compared to the broadening and shift of the glass transition of bulk semicrystalline PET samples. These are obtained by annealing amorphous samples at 100°C for prolonged times (Fig. 4).

A prolonged time for cold crystallization at 100°C leads to bulk PET samples with an increased crystallinity. Concomitant with the reduction of the amount of the amorphous fraction, as can be observed from the reduction in $\Delta Cp$ at the $T_g$ from about 0.37 to about 0.28 $Jg^{-1}\,°C^{-1}$, the amorphous phase also becomes less mobile. The derivative of the *Cp* signal shows, indeed, a shift of the $T_g$ to higher temperatures. A second, much broader peak, centered at about 90°C, appears. At an annealing time of 3 h, the sharp peak in the *dCp/dT* signal below 80°C almost disappears, and at an annealing time of 6 h, only the second, broad transition is visible. For the longest annealing times, still another peak above the annealing temperature is observed. This step in *Cp* is probably due to the melting of unstable crystals formed during the annealing treatment. The nonreversing signal indeed shows a start of recrystallization at this temperature. Also, a further annealing of the samples at temperatures of, respectively, 130, 140, and 150°C for only 2 min results in a shift of the latter step in *Cp* and the onset of recrystallization in the noneversing heat-flow signal to a tem-

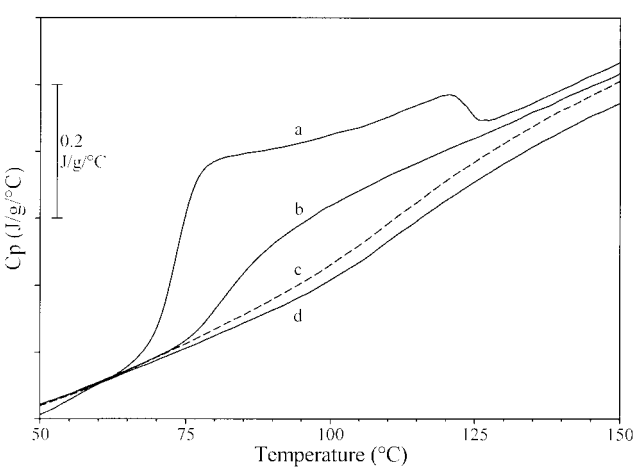


**Figure 3** Glass transition region of bulk and fibrous PET. MDSC: (a) Amorphous bulk sample; (b) semicrystalline bulk sample; (c) microfiber; (d) conventional fiber.

**TABLE I**
**Glass Transition Temperature ($T_g$), Onset Temperature of the Glass Transition Region ($T_{g_{onset}}$), Endset Temperature of the Glass Transition Region ($T_{g_{endset}}$), and the Step in Heat Capacity at the Glass Transition ($\Delta Cp$) of the PET Conventional Fibers and Microfibers**

| Sample | $T_{gonset}$ (°C) | $T_g$ (°C) | $T_{gendset}$ (°C) | $\Delta Cp$ (J $g^{-1}$ $°C^{-1}$) |
|---|---|---|---|---|
| Weft conventional fiber | 96 | 112 | 130 | 0.21 |
| Warp conventional fiber | 102 | 114 | 130 | 0.17 |
| Weft microfiber | 96 | 109 | 126 | 0.20 |
| Warp microfiber | 98 | 111 | 127 | 0.17 |

perature around the respective annealing temperature (not shown). Similar effects of the heat-set process are noticed around the heat-set temperature (see Fig. 8 and 10).

Figure 4 also shows that the $T_g$ of the fibers is shifted to even higher temperatures and the $\Delta Cp$ is smaller than any of the annealed bulk samples. The $T_g$ of the microfiber and of the conventional fiber are similar (see also Fig. 3 and Table I). Slight differences in the glass transition between both fibers are not unexpected as a result of different production parameters of fibers with another diameter. Variations in production parameters may also result in more substantial variations in the fiber $T_g$ (see original yarns in Table II). The differences between the two fibers shown here are, however, small compared to the differences between the fibers and the bulk PET samples annealed for various times.

It should be noted that, similar to the bulk PET sample annealed for 24 h, the very broad peak in the *dCp/dT* signal of the fibers is situated after the sharp maximum of the fully amorphous sample around 70°C. By analogy with the results of Song and Hourston,[28] this may suggest the presence of a high amount

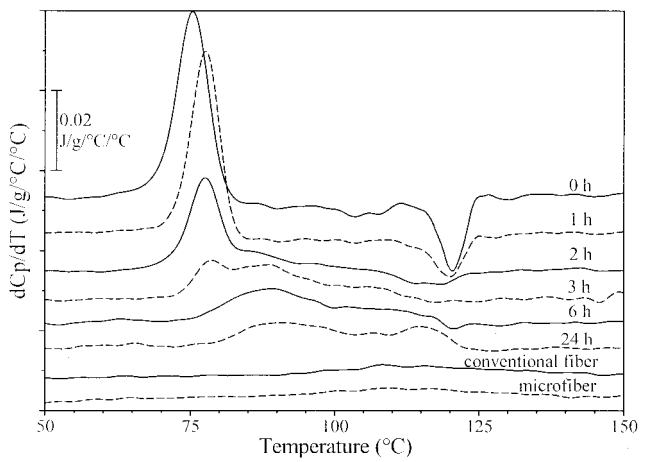


**Figure 4** Variations in glass transition of fibrous PET samples and bulk PET samples prepared by annealing bulk amorphous PET samples for prolonged times (0–24 h) at 100°C. MDSC.

of a rigid amorphous phase and almost no bulk amorphous phase in the noncrystalline phase of the fiber. For the bulk PET, the rigid amorphous phase is caused by the introduction of small crystals during the annealing treatment. In the fibers, however, the drawing and resulting molecular orientation play an important role in the increase of crystallinity and decrease of mobility of the amorphous phase.

### Characterization of the melting transition

Figure 5 shows a zoom of Figure 1 in the melting transition region. A multiple melting endotherm for the fibers is observed, which is different from the melting of the bulk semi-crystalline PET sample.

The multiple melting of bulk PET has been widely studied by conventional DSC, in many cases using varying heating rates. Groeninckx et al. observed single or double melting endotherms for bulk PET samples,[12,13] depending on the thermal history of the sample and the heating rate. In the case of double melting peaks, the first endotherm is attributed to the melting of the original crystalline material, whereas the second endotherm is attributed to the melting of crystalline material reorganized during the DSC scan. On sufficiently slow heating, continuous perfection of the original spherulites occurs through repeated recrystallization.[31,32] Therefore the high-temperature melting peak is due to the continuously perfecting and recrystallizing material. Several authors reported a triple melting behavior of bulk PET samples.[14–17] The first and second melting endotherms are assigned to the melting of originally present secondary and or primary crystals. The third melting endotherm is assigned to the melting of crystals reorganized during the DSC scan. Using MDSC, it was shown that the reorganization already starts at the first endotherm.[15]

On the contrary, little has been reported on the melting of PET fibers. Fakirov et al.[33] observed a double-melting behavior on both drawn and undrawn PET bristles, which they attributed to a melting and recrystallization process. They attributed the differences between drawn and undrawn samples to different crystallization kinetics. Elenga et al.[34] also ob-

**TABLE II**
**$T_g$, $T_{g_{onset}}$, $T_{g_{endset}}$, $\Delta Cp$ at $T_g$ (Heat-capacity Signal) and Onset Temperature of Melting and Recrystallization (Nonreversing Heat-flow Signal) for the Fabric Qualities 6645, 6447, and 5065 as a Function of Heat-set Temperature**

| Fabric quality | Programmed heat-set temperature (°C) | | $T_{gonset}$ (°C) | $T_g$ (°C) | $T_{gendset}$ (°C) | $\Delta Cp$ (J $g^{-1}$ $°C^{-1}$) | Onset of melting and recrystallization (°C) |
|---|---|---|---|---|---|---|---|
| Weft, 6645 | Original yarn | | 77 | 100 | 121 | 0.27 | 78 |
| | Dried at | 140°C | 100 | 111 | 122 | 0.23 | 108 |
| | | 180°C | 96 | 114 | 130 | 0.21 | 173 |
| | | 200°C | 98 | 113 | 129 | 0.18 | 195 |
| | | 220°C | 87 | 106 | 125 | 0.23 | 208 |
| Warp, 6645 | Original yarn | | 100 | 115 | 131 | 0.20 | 133 |
| | Dried at | 140°C | 101 | 114 | 130 | 0.21 | 146 |
| | | 180°C | 98 | 114 | 131 | 0.19 | 175 |
| | | 200°C | 98 | 113 | 129 | 0.19 | 195 |
| | | 220°C | 93 | 110 | 128 | 0.21 | 206 |
| Weft, 6447 | Original yarn | | — | — | — | — | — |
| | Dried at | 140°C | 100 | 118 | 140 | 0.29 | 128 |
| | | 180°C | 96 | 112 | 128 | 0.20 | 173 |
| | | 200°C | 95 | 111 | 127 | 0.18 | 190 |
| | | 220°C | 89 | 109 | 125 | 0.23 | 196 |
| Warp, 6447 | Original yarn | | 98 | 114 | 132 | 0.21 | 130 |
| | Dried at | 140°C | 102 | 116 | 133 | 0.22 | 130 |
| | | 180°C | 94 | 111 | 128 | 0.22 | 173 |
| | | 200°C | 91 | 109 | 125 | 0.22 | 189 |
| | | 220°C | 92 | 110 | 125 | 0.21 | 201 |
| Weft, 5065 | Original yarn | | 97 | 113 | 132 | 0.22 | 150 |
| | Dried at | 140°C | 102 | 115 | 130 | 0.21 | 150 |
| | | 180°C | 101 | 115 | 130 | 0.18 | 169 |
| | | 200°C | 91 | 112 | 130 | 0.22 | 190 |
| | | 220°C | 94 | 111 | 125 | 0.20 | 215 |
| Warp, 5065 | Original yarn | | 78 | 102 | 124 | 0.30 | 78 |
| | Dried at | 140°C | 105 | 118 | 132 | 0.19 | 115 |
| | | 180°C | 102 | 115 | 130 | 0.18 | 170 |
| | | 200°C | 99 | 114 | 126 | 0.17 | 186 |
| | | 220°C | 93 | 111 | 126 | 0.19 | 209 |

served a double-melting behavior on drawn PET samples but interpreted this in terms of morphological changes induced by drawing instead of recrystallization. Miyagi and Wunderlich[35] showed that PET fibers drawn from the melt reorganize on slow heating when unrestrained.

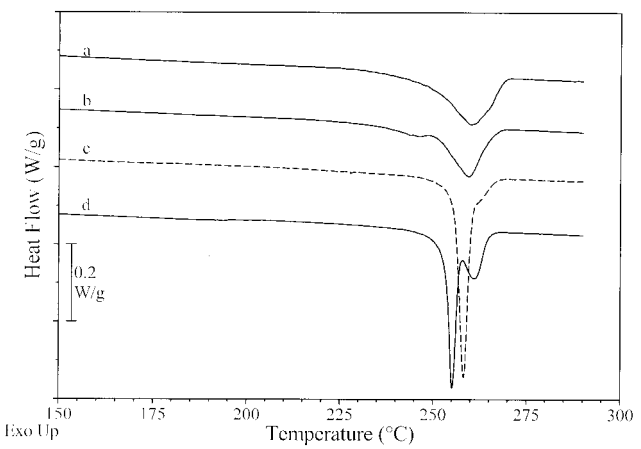


**Figure 5** Melting region of bulk and fibrous PET samples. Conventional DSC. (a) Amorphous bulk sample; (b) semicrystalline bulk sample; (c) microfiber; (d) conventional fiber.

Figure 6 shows the multiple-melting behavior with varying heating rates of the weft fibers of the basic conventional fiber PET fabric and bulk semicrystalline PET samples obtained from the conventional PET fiber after cooling from the melt at 20°C/min. All melting peaks of the fiber shift to higher temperatures with a decreasing heating rate, although the shift is a little bigger for the highest-temperature melting endotherm. This suggests that the whole multiple melting profile observed on the fibers is the result of a continuous melting and recrystallization process and not only the highest-temperature endotherm. The semicrystalline bulk PET samples in Figure 6 behave as was observed in most of the literature for bulk PET,[12–17] with only the highest-temperature endotherm shifted to higher temperatures with a decreasing heating rate.

The suggested continuous melting and recrystallization process for the conventional PET fibers is also

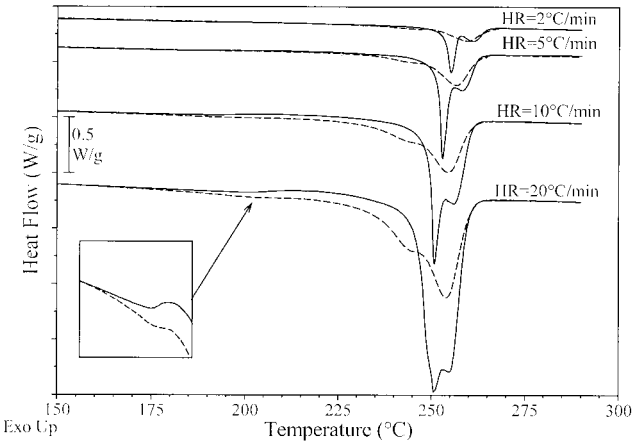


**Figure 6** Melting region of bulk and fibrous PET samples. Conventional DSC with varying heating rate: 2–20°C/min. (____) Conventional fiber, (- - - -) semi-crystalline bulk sample.

observed for the microfibers, as shown in Figure 7. The multiple-melting behavior is, however, not as obvious. The variation in the melting profile of both fibers is due to the different morphology of the fibers, as a result of their distinct spinning conditions. The microfibers show a narrower melting endotherm at a temperature in between the two melting endotherms of the conventional fibers (Fig. 5). Apart from a shift of this endotherm to higher temperatures with a decreasing heating rate, a very weak higher-temperature melting endotherm can be observed at low heating rates, whereas at higher heating rates, the narrow melting endotherm broadens to lower temperatures, which agrees with the proposed continuous melting and recrystallization process during the DSC scan.

The recrystallization in the fibers can be confirmed with MDSC, as shown in Figure 8 for the microfibers. The start of recrystallization is observed as an exotherm in the nonreversing heat-flow signal with an onset around 170°C. The *Cp* signal shows a small step

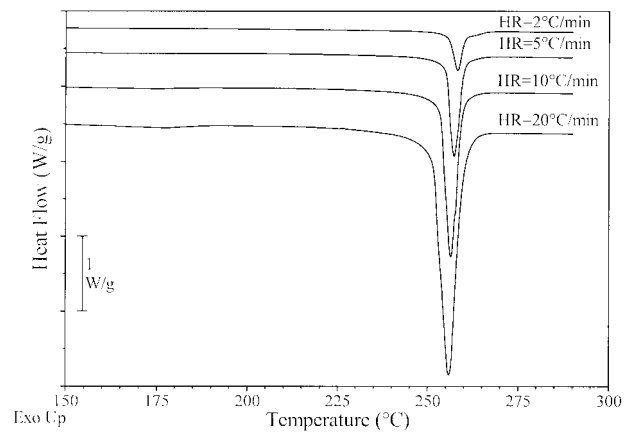


**Figure 7** Melting region of PET microfibers. Conventional DSC with varying heating rate: 2°–20°C/min.

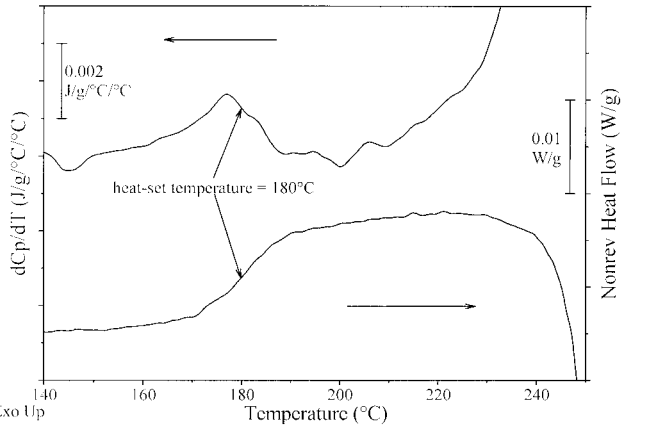


**Figure 8** Start of melting and recrystallization of PET microfibers. MDSC.

with an onset around 165°C and endset around 185°C, more visible in the *dCp/dT* signal as a small peak. This is assigned to an excess *Cp* as a result of the start of melting and recrystallization.

The melting and recrystallization process thus starts at a temperature somewhat lower than the heat-set temperature of the fabrics. It is important to notice that an industrial heat-set treatment at 180°C means a temperature of 180°C at the heating plates of the stenter. The temperature in the fabric, which is still a couple of centimeters away from the heating plates and is only exposed to the heat source for 30 s, may thus not reach 180°C. The onset of melting and recrystallization around 170°C, in this case, may thus possibly be related to the real heat-set temperature in the fabric. The exposure time will, however, also influence this onset temperature. Similarly, the annealing of bulk PET samples results in the onset of melting and recrystallization at a temperature near to the annealing temperature[15] (see the longest annealing times in Fig 4). This may thus suggest that for fibers the melting and recrystallization process is triggered by the heat-set treatment. This is discussed further on (Fig. 10 and Table II).

The start of the melting and recrystallization process in the fibers can also be observed in the higher heating rate curves of Figure 6 (see inset) as a very weak exotherm. The onset of the exotherm increases with the heating rate as a result of "superheating." In the highest heating rate curve of the bulk sample, a weak and broad endotherm can be observed, which is in agreement with the literature.[15] So, in the bulk samples studied, the net effect of melting and recrystallization is a weak endotherm, whereas it is a weak exotherm in the fibers.

In contrast to bulk PET, little is known on the crystal morphology of PET fibers, with the fiber-spinning conditions affecting this morphology. In this work, fibers from commercially available fabrics were used

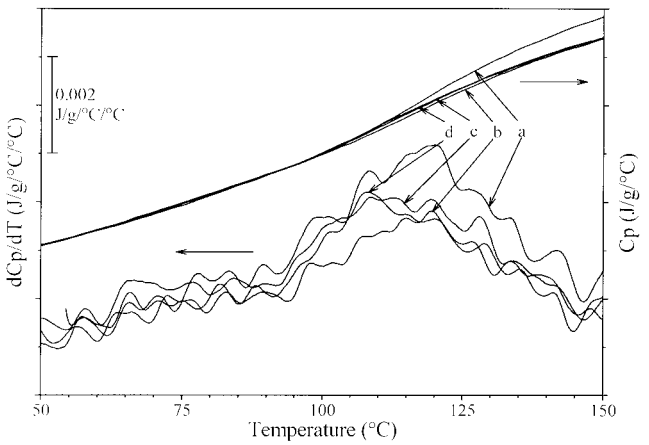


**Figure 9** Variations in glass transition with varying heat-set temperature for warp fibers of fabric quality 6645. MDSC: (a) Dried at 140°C; (b) heat-set at 180°C; (c) heat-set at 200°C; (d) heat-set at 220°C.

to perform a realistic dyeing process. The yarns to produce the fabrics were from different suppliers and the specific fiber production parameters were kept confidential. There are, therefore, many unknown parameters and it is not possible at this stage to make any further statements on whether the multiple melting observed in the fibers is only the result of a melting and reorganization process or whether there is also an initial dual distribution of the crystal morphology as is suggested for bulk PET.[12–17] It is, however, clear that the start of the melting and reorganization process for the standard fabric qualities studied here is well above the dyeing temperature, which is necessary for a dimensionally stable dyed fabric.

### Effect of the heat-set temperature on the glass transition and the start of melting and recrystallization

To gain a better understanding of the effect and importance of the heat-set process on the thermal properties and thus also the dyeing or other high-temperature processing properties of PET fibers, three series of fabrics, heat-set at different temperatures (180, 200, and 220°C) were investigated. The original warp and weft yarns of the fabrics as well as a fabric that did not receive a heat-set treatment but only the preliminary drying treatment at 140°C were also studied.

Figure 9 shows the glass transition region, monitored by MDSC, for the warp fibers of fabric quality 6645. Table II gives an overview of the glass transition characteristics (measured on the *Cp* signal) and the onset of melting and recrystallization (measured on the nonreversing heat-flow signal) for warp and weft of all three fabric qualities as a function of the heat-set temperature.

Figure 9 and Table II indicate that the heat-set temperature affects the glass transition of the fibers, although the variations in the glass transition with the heat-set temperature are not as obvious for all fiber samples. Probably, the original fiber morphology determined by the specifications of the fiber production processes is an important parameter in this feature. The study of the thermal properties of these original yarns reveals that both the 6645 weft yarn and the 5065 warp yarn show a major difference in the glass transition compared to the other yarns. Note that the onset of melting and recrystallization (Table II) for these two yarns coincides with the onset of the $T_g$. This low onset temperature suggests that these yarns did not receive a high-temperature setting treatment as part of their production process. Due to the overlap of both processes, the $T_g$ region may be expanded due to a changing morphology during the heating. This may result in overestimated endset temperatures of $T_g$ and $\Delta Cp$ values. For some of the dried samples, the onset of melting and recrystallization was situated in the $T_g$ region, resulting in a similar overestimation.

However, some general trends may still be observed. A reduction in the glass transition temperature is effected by an increased heat-set temperature compared to the dried sample. This is substantial (around 5°C) for all fibers at the highest heat-set temperature of 220°C, whereas the $T_g$ reduction at lower heat-set temperatures seems to be more dependent on the original fiber morphology. $\Delta Cp$ at the $T_g$ is also reduced but tends to reach a minimum at an intermediate heat-set temperature, after which it may slightly increase again.

The heat-set process can be regarded as a very short annealing treatment during which some melting and recrystallization will occur for the least stable crystals as well as some crystallization of the amorphous regions leading to a reduced $\Delta Cp$ at the $T_g$ for most samples. The slight increase in $\Delta Cp$ for some samples after a heat-set process at 220°C may be interpreted as a more obvious melting, which results in some material that cannot recrystallize. A temperature of 220°C is indeed already near to the start of a net melting as can be observed for the dried sample in Figure 10. Further, the decrease in the fiber $T_g$ suggests that the heat-set process also results in a partial relaxation of the amorphous regions. This is again more evident for the highest heat-set temperature since more material will have melted.

To fully understand the variations in the fiber $T_g$ with the heat-set temperature, more information is needed on the original fiber morphology and the fiber production specifications, but, as stated earlier, this is not possible for commercially available fabrics used for dyeing. It is, however, clear so far that the specifications of the heat-set process will affect the glass transition of the fiber and, as such, also the dyeing

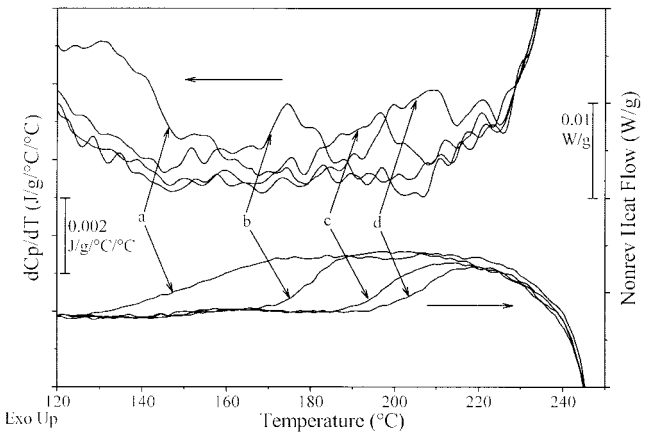


**Figure 10** Variations in onset of melting and recrystallization with varying heat-set temperature for weft fibers of fabric quality 6447. MDSC. (a) Dried at 140°C; (b) heat-set at 180°C; (c) heat-set at 200°C; (d) heat-set at 220°C.

properties. Further, the results show that a stable and uniform heat-set process is of utmost importance for the levelness of the dyed fabrics. Indeed, local variations in the fiber $T_g$ across the fabric will result in local differences in dye diffusion and color buildup. Moreover, microfiber fabrics are already prone to unlevel dyeings due to their often high fabric density and resulting lower uniform accessibility of the dyebath in the fabrics.[1]

The effect of the heat-set process on the onset of melting and recrystallization is illustrated in Figure 10 for the weft fibers of fabric quality 6447. The nonreversing heat-flow signal and the first derivative of the heat-capacity signal obtained with MDSC are shown. Similar to Figure 8, the nonreversing heat flow signal shows an onset of crystallization at a temperature near to the heat-set temperature. The *dCp/dT* signal also shows a small peak around the heat-set temperature. The onset of melting and recrystallization, as observed by both signals, indeed shifts to higher temperatures with higher heat-set temperatures, confirming the earlier suggested triggering of melting and recrystallization by the heat-set process. Table II confirms this for all of the fibers tested.

These results demonstrate that MDSC is a sensitive technique for monitoring the heat-set temperature history of PET fabrics. It is, however, clear from the above that it will not give the exact programmed heat-set temperature but the start temperature of the melting and recrystallization process and this will vary not only with heat-set temperature but also with other process conditions, such as fabric speed through the stenter, specifications of heat exchange, and fabric structure.

## CONCLUSIONS

It has been demonstrated that MDSC is a useful technique to monitor the very broad and weak glass transition of PET fibers, which cannot be revealed by conventional DSC. The high molecular orientation and high degree of crystallinity of the fibers results in a decrease of the mobility of the amorphous phase and a concomitant broad and weak glass transition (with an onset at ca. 100°C and an endset at ca. 130°C), shifted to higher temperatures compared to amorphous bulk PET (with a sharp transition around 70°C). The fiber $T_g$ is found to be even weaker and situated at higher temperatures than the $T_g$ of the bulk amorphous PET samples annealed for 24 h at 100°C. The endset of the glass transition of both the conventional fibers and the microfibers around 130°C provides evidence for the first time that the empirically determined dyeing temperature of 130°C is appropriate to a first approximation. The temperature of the dyebath indeed needs to be increased above the fiber $T_g$ for most of the amorphous phase to become mobile, allowing for an efficient diffusion of dye into the fiber and thus also proper color buildup. As such, MDSC serves well as a technique to understand and possibly optimize the dyeing process.

There remain, however, more subtle differences in the glass transition of different fibers. These can be due to an original difference in the fiber morphology due to different spinning conditions during the production of the fibers. The subsequent heat-set process to which most fabrics are exposed prior to dyeing also plays an important role for the eventual glass transition of the fibers and thus also for the dye diffusion and concomitant color buildup of the fabrics. Variations in the heat-set temperature will give rise to variations in the fiber $T_g$. As such, the optimization of the heat-set process is of utmost importance for the dyeing quality of the fabrics. Not only should the temperature be well chosen, it should also be uniform across the fabric, as it may, otherwise, lead to local differences in dye diffusion and thus unlevel dyeings. MDSC serves as a sensitive tool for monitoring these differences and offers the potential for optimizing the dyeing process, which, until recently, depended on empirical methods.

Although the glass transition is the most direct significant thermal property for the dyeing performance of a fiber, the melting transition is also important as it determines the dimensional stability during any high-temperature process. The study of the melting transition of the fibers by conventional DSC reveals that the whole multiple melting profile is the result of a continuous melting and recrystallization process. This is in contrast to bulk PET samples where only the highest-temperature melting peak is attributed to the melting of reorganized crystals.

Further MDSC experiments show that the heat-set temperature triggers the start of this melting and recrystallization process. The (empirically determined) heat-set temperature around 180°C is sufficient to

push the start of melting well above the dyeing temperature, thus ensuring the dimensional stability during dyeing. Microfiber fabrics are often subjected to a coating process, which is commonly performed at temperatures around 160–180°C. It is clear that the onset of melting and recrystallization is not only an important property for the dyeing process but also for ensuring the dimensional stability during any further high-temperature processes the fabrics are subjected to.

In this article, a methodology for determining the thermal properties of PET fibers was established. In a following article,[21] this methodology will be exploited to investigate the interrelation between dyeing with various disperse dyes and these thermal properties.

Part of this work was funded by the European Commission through the Growth Program (Project Contract BRPR-CT98-0793) and by Ghent University (Ph.D. Grant 011D5495).

## References

1. Burkinshaw, S. M. Chemical Principles of Synthetic Fiber Dyeing; Chapman & Hall: Glasgow, 1995; Chapter 4.
2. Leadbetter, P.; Dervan, S. J Soc Dyers Colour 1992, 108, 369.
3. Griesser, W.; Tiefenbacher, H. Textilveredlung 1993, 28(4), 88.
4. Wiegner, D. Melliand Textilber 1992, 73, 743.
5. Dupeuble, J.-C. Man-Made Fiber Year Book; Chemiefasern/Textilindustrie: Frankfurt, 1991; p 88.
6. Rubin, B.; Kobsa, H.; Shearer, S. M. Text Res J 1993, 63, 685.
7. Chao, Y. C.; Chen, S. S. Dyes Pigments 1994, 24, 205.
8. Peters, R. H. Textile Chemistry, Vol. III, The Physical Chemistry of Dyeing; Elsevier: Amsterdam, 1975; p 713.
9. Ingamells, W. C. In The Theory of Coloration of Textiles; Johnson, A., Ed.; Society of Dyers and Colourists: Bradford, 1989; p 204.
10. Burkinshaw, S. M. Chemical Principles of Synthetic Fiber Dyeing; Chapman & Hall: Glasgow, 1995; Chapter 1.
11. Brennan, C. M.; Bullock, J. F. In Advances in Color Chemistry, Vol. 4, Physico-chemical Principles of Color Chemistry; Peters, A. T.; Freeman, H. S., Eds.; Chapman & Hall: Glasgow, 1996; Chapter 2.
12. Groeninckx, G.; Reynaers, H.; Bergmans, H.; Smets, G. J Polym Sci Polym Phys Ed 1980, 18, 1311.
13. Groeninckx, G.; Reynaers, H. J Poly Sci Polym Phys Ed 1980, 18, 1325.
14. Zhou, C.; Clough, S. B. Polym Eng Sci 1988, 28, 65.
15. Wang, Z. G.; Hsiao, B. S.; Sauer, B. B.; Kampert, W. G. Polymer 1999, 40, 4615.
16. Medellin-Rodriguez, F. J.; Phillips, P. J.; Lin, J. S.; Campos, R. J Polym Sci Part B Polym Phy 1997, 35, 1757.
17. Medellin-Rodriguez, F. J.; Phillips, P. J.; Lin, J. S. Macromolecules 1996, 29, 7491.
18. Toda, A.; Tomita, C.; Hikosaka, M.; Saruyama, Y. Polymer 1998, 39, 5093.
19. Okazaki, I.; Wunderlich, B. Macromolecules 1997, 30, 1758.
20. Schick, C.; Merzlyakov, M.; Wunderlich, B. Polym Bull 1998, 40, 297.
21. De Clerck, K.; Rahier, H.; Van Mele, B.; Kiekens, P., submitted *for publication in* J Appl Polym Sci.
22. Swier, S.; Van Assche, G.; Van Hemelrijck, A.; Rahier, H.; Verdonck, E. Van Mele, B. J Therm Anal 1998, 54, 585.
23. Encyclopedia of Polymer Science and Engineering; Kroschwitz, J. I.; Klingsberg, A.; Piccininni, R.; Salvatore, A.; Baldwin, T., Eds.; John Wiley & Sons: New York; Vol. 12, p 127.
24. Fu, Y.; Annis, B.; Boller, A.; Jin, Y.; Wunderlich, B. J Polym Sci Part B Polym Phys 1994, 32, 2289.
25. Fu, Y.; Busing, W. R.; Jin, Y.; Affholter, K. A.; Wunderlich, B. Macromol Chem Phys 1994, 195, 803.
26. Suzuki, H.; Grebowicz, J.; Wunderlich, B. Brit Polym J 1985, 17, 1.
27. Mathot, V. B. F. In Calorimetry and Thermal Analysis of Polymers, Mathot, V. B. F., Ed.; Hanser: Munich, 1994; Chapter 5.
28. Song, M.; Hourston, D. J. J Therm Anal 1998, 54, 651.
29. Jones, K. J.; Kinshott, I.; Reading, M.; Lacey, A. A.; Nikolopoulos, C.; Pollock, H. M. Thermochem Acta 1997, 304/305, 187.
30. De Meuter, P.; Amelrijckx, J.; Rahier, H.; Van Mele, B. J Polym Sci Part B Polym Phys 1999, 37, 2881.
31. Zachmann, H. G.; Stuart, H. A. Macromol Chem 1960, 8, 131.
32. Wunderlich, B. Macromolecular Physics, Vol. 3, Crystal Melting; Academic: New York, 1980; p 181.
33. Fakirov, S.; Fischer, E. W.; Hoffman, R.; Schmidt, G. F. Polymer 1977, 18, 1121.
34. Elenga, R., Seguela, R.; Rietsch, F. Polymer 1991, 32, 1975.
35. Miyagi, A.; Wunderlich, B. J Polym Sci Polym Phys Ed 1972, 10, 1401.